

Application of Zn + p reactions for production of copper radioisotopes for medical studies

F. Szelecsényi^{1,a}, G.F. Steyn², K. Suzuki³, Z. Kovács¹, T.N. van der Walt², C. Vermeulen², N.P. van der Meulen², S.G. Dolley², and K. Mukai³

¹ Institute of Nuclear Research of the Hungarian Academy of Sciences (ATOMKI), 4026, Bem tér 18/C, Debrecen, Hungary

² iThemba Laboratory for Accelerator Based Sciences, Old Faure Road, P.O. Box 722, Somerset West 7129, South Africa

³ National Institute of Radiological Sciences, 4-9-1 Anagawa, Inage-ku, Chiba, 263-8555, Japan

Abstract. The production possibility of four medically important copper radioisotopes via Zn + p reactions was studied up to 80 MeV. Based on experimentally evaluated excitation function curves of the $^{64}\text{Zn}(p,x)^{61}\text{Cu}$, $^{\text{nat}}\text{Zn}(p,x)^{62}\text{Zn} \rightarrow ^{62}\text{Cu}$, $^{66}\text{Zn}(p,2p)^{64}\text{Cu}$, $^{68}\text{Zn}(p,x)^{64}\text{Cu}$ and $^{68}\text{Zn}(p,2p)^{67}\text{Cu}$ reactions, production energy windows are recommended for the ^{61}Cu , ^{62}Cu , ^{64}Cu and ^{67}Cu isotopes. The available yields for these radioisotopes as well as the predicted yields of the major radiocontaminants are also presented.

1 Introduction

Radiopharmaceuticals labelled with different copper radioisotopes are becoming increasingly important for PET studies as well as for radiotherapy. At present, the routine production of these radioisotopes (^{61}Cu [$T_{1/2} = 3.3$ h], ^{62}Cu [$T_{1/2} = 9.7$ min], ^{64}Cu [$T_{1/2} = 12.7$ h] and ^{67}Cu [$T_{1/2} = 61.8$ h]) are based mainly on charged particle induced nuclear reactions on highly enriched and very expensive Ni targets (see, e.g., refs. [1,2] and references therein). Recently, extensive new investigations have been initiated to find alternative methods which also form these radio-coppers with efficient yields, but employing cheaper enriched target materials. Promising candidates are the Zn + p and Co + α reactions below 100 MeV. A review on the Co + α route was recently published in ref. [3]. It was found, however, that the production related nuclear data for the Zn + p reactions were either scanty or rather discrepant. Consequently, the available information was not sufficient to calculate production yields and radio-impurity concentrations with the required precision. To clarify the above problems, we report here on our recent results on the following nuclear reactions: $^{64}\text{Zn}(p,x)^{61}\text{Cu}$, $^{\text{nat}}\text{Zn}(p,x)^{62}\text{Zn} \rightarrow ^{62}\text{Cu}$, $^{68}\text{Zn}(p,x)^{64}\text{Cu}$, $^{66}\text{Zn}(p,2p)^{64}\text{Cu}$, and $^{68}\text{Zn}(p,2p)^{67}\text{Cu}$ from their respective threshold energies up to a maximum of 80 MeV.

2 Experimental

Natural and highly enriched zinc targets were activated with proton beams supplied by cyclotrons of ATOMKI (Debrecen), iThemba LABS (Faure) and NIRS (Chiba). The cross sections were measured by means of the conventional stacked-foil method. The activities induced in the irradiated samples were measured using conventional off-line γ -ray spectroscopy. In selected cases, chemical separation of the Cu from the Zn was first performed. The experimental details are described in refs. [4–7].

^a Present author, e-mail: szele@atomki.hu

3 Results and discussion

The investigated nuclear reactions suggested for production purposes are ordered according to increasing mass number of the residual nucleus. The excitation function curves shown in figures 1, 3, 5 and 7 were created by means of cubic-spline fits through our measured cross sections as well as those of acceptable literature data sets, where applicable (for details, see refs. [4–7]). The thick-target yield calculations (shown in figs. 2, 4, 6 and 8) were derived from these curves. During the activation of Zn with protons up to 80 MeV, the formation of several gallium, zinc, nickel and cobalt radioisotopes also occurs. From a production point of view, however, the presence of these radioisotopes in the activated targets does not constitute a major problem. Methods for the effective separation of Cu, Ga, Ni and Co from a Zn matrix (and from each other) have been published in numerous articles in the past. As a result, several quick and automated methods are available to isolate Cu cleanly. In addition to the cross section measurements, we have also elaborated on a new efficient method for the separation of $^{64,67}\text{Cu}$ from a bulk Zn matrix [8].

3.1 Production of ^{61}Cu

Our candidate for routine production of ^{61}Cu is the $^{64}\text{Zn}(p,x)^{61}\text{Cu}$ nuclear process. Numerous reactions (direct reactions and reactions through decays of the co-produced ^{61}Ga [$T_{1/2} = 0.15$ s] ($^{64}\text{Zn}(p,4n)^{61}\text{Ga} \rightarrow ^{61}\text{Zn} \rightarrow ^{61}\text{Cu}$) and ^{61}Zn [$T_{1/2} = 89.1$ s] ($^{64}\text{Zn}(p,p3n)^{61}\text{Zn} \rightarrow ^{61}\text{Cu}$), contribute to the formation of ^{61}Cu up to 80 MeV. Below 30 MeV, mainly the $^{64}\text{Zn}(p,\alpha)$ reaction contributes to ^{61}Cu formation while above this energy the (p,2p2n) process becomes dominant. The excitation function curve of this process (see fig. 1) shows two peaks: a local maximum of 84 mb at 14.5 MeV and another of 139 mb at 54.5 MeV.

Activation of ^{64}Zn could form two other longer-lived copper radioisotopes (^{60}Cu [$T_{1/2} = 23.2$ min] and ^{62}Cu). From a radionuclide production point of view, the ^{60}Cu can be

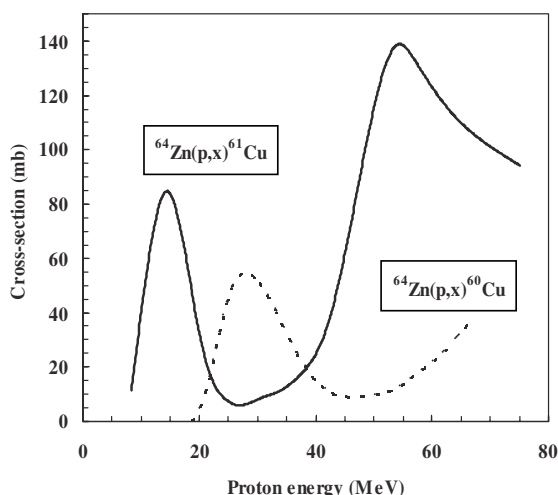


Fig. 1. Excitation functions of the $^{64}\text{Zn}(p,x)^{60}\text{Cu}$ and $^{64}\text{Zn}(p,x)^{61}\text{Cu}$ nuclear processes.

considered as the major contaminant. The excitation function curve of the $^{64}\text{Zn}(p,x)^{60}\text{Cu}$ process is also shown in figure 1 (contributing reactions: $^{64}\text{Zn}(p,\alpha n)^{60}\text{Cu}$, $^{64}\text{Zn}(p,2p3n)^{60}\text{Cu}$, $^{64}\text{Zn}(p,5n)^{60}\text{Ga} \rightarrow ^{60}\text{Zn} \rightarrow ^{60}\text{Cu}$ and $^{64}\text{Zn}(p,p4n)^{60}\text{Zn} \rightarrow ^{60}\text{Cu}$). This process has one peak below 80 MeV (at about 28.5 MeV with a maximum of 54 mb). Using the excitation function curves of figure 1, integral thick-target yields were calculated up to 70 MeV. The results are plotted in figure 2. By analyzing these results, it can be concluded that two energy windows can be employed for routine production of ^{61}Cu . At a low energy cyclotron, 19 → 10 MeV, the available yield is 9.9 mCi/μAh with 0.05 mCi/μAh ^{60}Cu contamination at the end of bombardment (EOB). Having higher proton energies, one can use an energy window of 67 → 60 MeV, where the available yield amounts to 38 mCi/μAh. In the latter case, however, a substantial amount of ^{60}Cu (and ^{62}Cu) is also formed. The percentage of this contamination strongly depends on the actual irradiation time. Assuming a 1 h irradiation time, the activity of ^{60}Cu reaches 86 mCi/μA at EOB. However, during the time of separation and labelling (3–4 h) the ^{60}Cu activity decays to an acceptable level (<1%).

3.2 Production of $^{62}\text{Zn}/^{62}\text{Cu}$ generator

The practical production of ^{62}Cu is based on the $^{62}\text{Zn}/^{62}\text{Cu}$ generator. Nowadays, ^{62}Zn [$T_{1/2} = 9.2$ h] is routinely produced via the $^{\text{nat}}\text{Cu} + p$ reaction [9]. However, at higher energies the $^{\text{nat}}\text{Zn}(p,x)^{62}\text{Zn}$ process could be a competitor. In the case of the $\text{Zn} + p$ route, the ^{62}Zn activity is a result of cumulative production. ^{62}Zn is formed in direct reactions and through the production of ^{62}Ga [$T_{1/2} = 116.1$ ms] that decays 100% to ^{62}Zn . Although seven reactions contribute to the formation of ^{62}Zn using a natural zinc target up to 70 MeV, mainly the $^{64}\text{Zn}(p,p2n)^{62}\text{Zn}$ reaction is dominant from the point of view of the shape of the excitation function curve (see fig. 3). The “cumulative” excitation function curve has a maximum of about 48 mb at 39 MeV.

Based on the above excitation function curve, we have calculated the expected integral thick-target yields for the

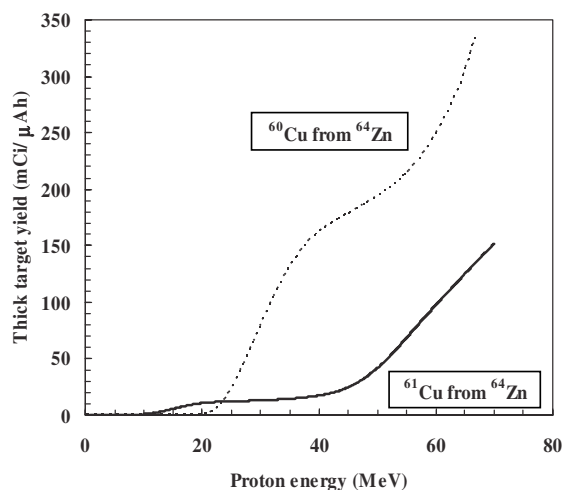


Fig. 2. Integral thick-target yields of the $^{64}\text{Zn}(p,x)^{60}\text{Cu}$ and $^{64}\text{Zn}(p,x)^{61}\text{Cu}$ nuclear processes.

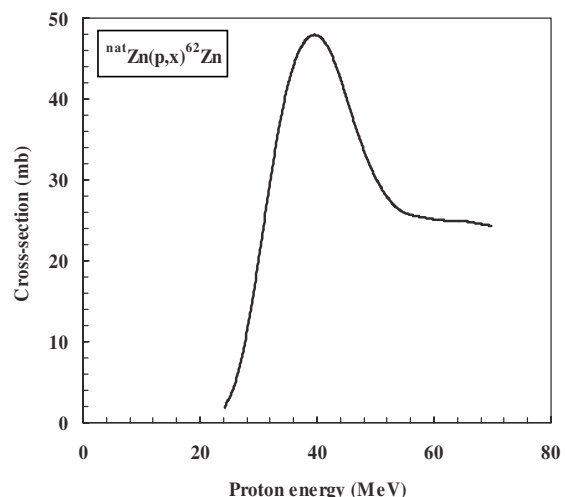


Fig. 3. Excitation function of the $^{\text{nat}}\text{Zn}(p,x)^{62}\text{Zn}$ nuclear process.

$^{\text{nat}}\text{Zn}(p,x)^{62}\text{Zn}$ process up to 70 MeV. These results are shown in figure 4. For comparison, we have also calculated the yield of the $^{\text{nat}}\text{Cu}(p,xn)^{62}\text{Zn}$ process using the recommended cross-section data presented in ref. [10]. On the basis of these calculations, it can be seen that the $^{\text{nat}}\text{Zn}(p,x)$ process produces more activity above 50 MeV than the $^{\text{nat}}\text{Cu}(p,xn)$ one. In the energy window from 70 down to 30 MeV, the available EOB yield is around 19 mCi/μAh. This value is 2.5 times higher than the yield from the $^{\text{nat}}\text{Cu}(p,xn)$ process in the same energy region.

Note that preparation of $^{62}\text{Zn}/^{62}\text{Cu}$ generators via the $\text{Zn} + p$ route is somewhat more complicated than in the case of the $\text{Cu} + p$ route. It needs more steps to separate the radioactive gallium, copper and nickel isotopes from the zinc matrix. However, these methods are well known, therefore the necessary separations can be done quickly and with high efficiency. As a result, high-purity ^{62}Zn can readily be obtained in the final product.

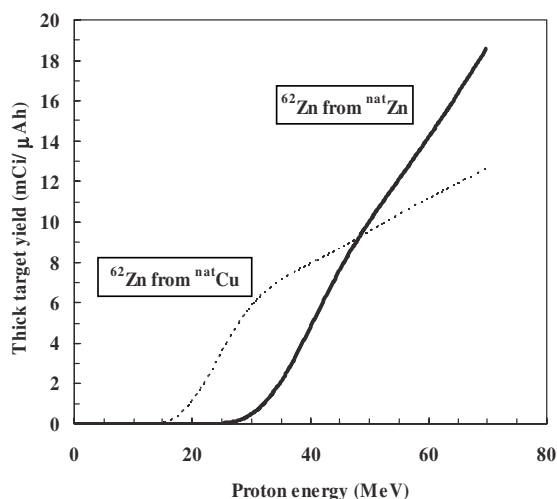


Fig. 4. Integral thick-target yields of the ${}^{\text{nat}}\text{Zn}(p,x){}^{62}\text{Zn}$ and ${}^{\text{nat}}\text{Cu}(p,x){}^{62}\text{Zn}$ nuclear processes.

3.3 Production of ${}^{64}\text{Cu}$

Both ${}^{66}\text{Zn}$ and ${}^{68}\text{Zn}$ targets can be used for practical ${}^{64}\text{Cu}$ production. In the case of ${}^{66}\text{Zn}$, only the ${}^{66}\text{Zn}(p,2pn)$ reaction forms the required radioisotope. The excitation function curve (shown in fig. 5) shows a peak at about 45 MeV with a maximum of 80 mb. The longest-lived radio-copper contamination in ${}^{64}\text{Cu}$ production is the ${}^{61}\text{Cu}$. It is formed via the ${}^{66}\text{Zn}(p,\alpha 2n)$ and ${}^{66}\text{Zn}(p,2p4n)$ reactions. As can be seen in figure 5, this excitation function curve peaks with a value of 46 mb at about 42 MeV. To evaluate the optimum production conditions, we have calculated the yields of ${}^{61}\text{Cu}$ and ${}^{64}\text{Cu}$. These results are plotted in figure 6. According to our calculations, a 21.0 mCi/ μAh EOB yield of ${}^{64}\text{Cu}$ is expected in the energy range from 70 to 35 MeV while for ${}^{61}\text{Cu}$ it is 32.8 mCi/ μAh . To reach a minimum ${}^{61}\text{Cu}$ contamination level of 1% at the time of administration, one has to wait at least 34 h (taking a 1 hour activation time into account). This way, the applicable yield will decrease to 3.3 mCi/ μAh . By using a higher bombarding energy, the available yield at EOB will increase, but consequently the required cooling period will also be much longer. Since the half-life of the contaminant is 3.7 times smaller than that of ${}^{64}\text{Cu}$, a product which is almost free from other Cu radioisotopes can be obtained after a proper cooling time. This is considered to be one of the main advantages of this method.

In the investigated energy region, two reactions contribute to the formation of ${}^{64}\text{Cu}$ on ${}^{68}\text{Zn}$. Below 36 MeV, only the ${}^{68}\text{Zn}(p,\alpha n){}^{64}\text{Cu}$ reaction channel is open but beyond this energy the ${}^{68}\text{Zn}(p,2p3n){}^{64}\text{Cu}$ reaction becomes dominant. The excitation function curve shows a first peak at about 26 MeV with a maximum of 64 mb (see fig. 7). After a minimum of 10 mb at about 40 MeV, the curve increases again with increasing energy. It reaches a second maximum near 70 MeV with a value of about 55 mb. Up to 80 MeV, both ${}^{61}\text{Cu}$ and ${}^{67}\text{Cu}$ are important as radio-contaminants. The ${}^{61}\text{Cu}$ is formed directly via the ${}^{68}\text{Zn}(p,\alpha 4n)$ reaction, while only the ${}^{68}\text{Zn}(p,2p)$ process produces ${}^{67}\text{Cu}$ below 70 MeV.

The excitation functions curves of the ${}^{68}\text{Zn}(p,x){}^{61}\text{Cu}$ and ${}^{68}\text{Zn}(p,2p){}^{67}\text{Cu}$ reactions are shown in figure 7. The first

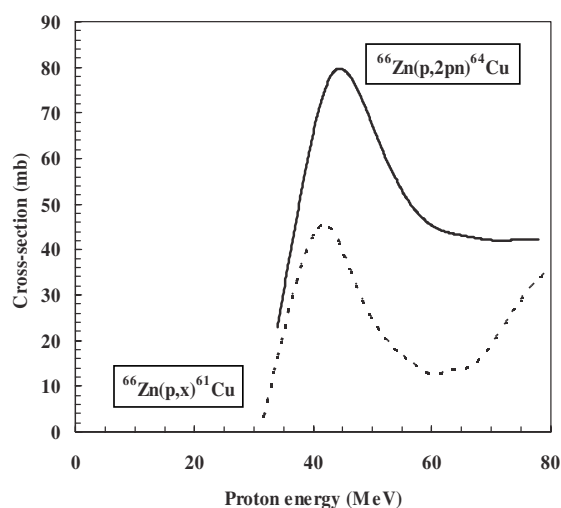


Fig. 5. Excitation functions of the ${}^{66}\text{Zn}(p,x){}^{61}\text{Cu}$ and ${}^{66}\text{Zn}(p,2pn){}^{64}\text{Cu}$ nuclear reactions.

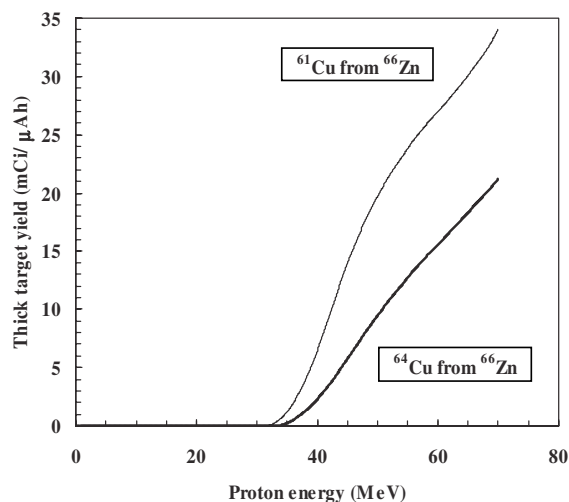


Fig. 6. Integral thick-target yields of the ${}^{66}\text{Zn}(p,x){}^{61}\text{Cu}$ and ${}^{66}\text{Zn}(p,x){}^{64}\text{Cu}$ nuclear processes.

reaction has a peak reaching a maximum of about 12 mb near 70 MeV. The latter one shows no peaks but increases monotonically up to 80 MeV. The integral thick-target yields of ${}^{61}\text{Cu}$, ${}^{64}\text{Cu}$ and ${}^{67}\text{Cu}$ calculated from their respective excitation functions are shown in figure 8. Since the formation of the longest-lived copper radioisotope, ${}^{67}\text{Cu}$, becomes significant at energies above 25 MeV, a ${}^{64}\text{Cu}$ yield of only about 1.8 mCi/ μAh at EOB is available in radio-copper contaminant-free form (in the production energy range 25 \rightarrow 10 MeV). By allowing a 0.9% ${}^{67}\text{Cu}$ contamination level at EOB, the available yield can be increased to 5.0 mCi/ μAh in the 37 \rightarrow 20 MeV energy range. Supposing a 5 h “application time” (for processing, PET study, etc.) the contamination level will remain at around 1% up to the end of this period. Although a significantly higher ${}^{64}\text{Cu}$ yield can be obtained above about 40 MeV, the ${}^{67}\text{Cu}$ contamination level will also increase as a function of energy. Above 55 MeV, ${}^{61}\text{Cu}$ will also be produced in the activated target.

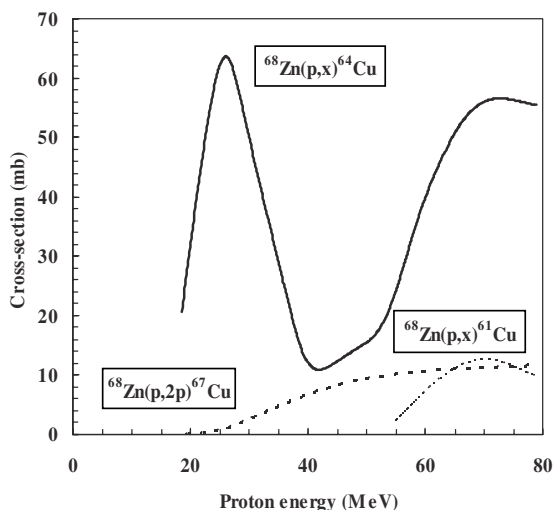


Fig. 7. Excitation functions of the $^{68}\text{Zn}(p,x)^{61}\text{Cu}$, $^{68}\text{Zn}(p,x)^{64}\text{Cu}$ and $^{68}\text{Zn}(p,2p)^{67}\text{Cu}$ nuclear processes.

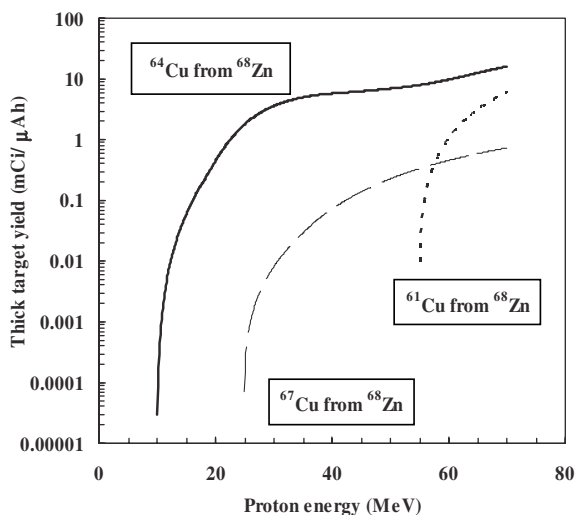


Fig. 8. Integral thick-target yields of the $^{68}\text{Zn}(p,x)^{61}\text{Cu}$, $^{68}\text{Zn}(p,x)^{64}\text{Cu}$ and $^{68}\text{Zn}(p,2p)^{67}\text{Cu}$ nuclear processes.

3.4 Production of ^{67}Cu

The behaviour of the excitation function curve of the $^{68}\text{Zn}(p,2p)$ nuclear reactions was already discussed in 3.3. Similarly, the thick-target yields of $^{61,64,67}\text{Cu}$ on ^{68}Zn was analyzed above. In the case of ^{67}Cu production, the ^{64}Cu is considered to be the main contamination. The expected yields (EOB) at 70 MeV are 0.76 and 16 mCi/ μAh for ^{67}Cu and ^{64}Cu , respectively. Taking into account the relatively long

half-life of ^{64}Cu , a major cooling period will be necessary in any production set-up before the medical application. Assuming a 1 h activation, the $^{64}\text{Cu}/^{67}\text{Cu}$ ratio will be <1% only after a 170 h cooling time. The practical yield, therefore, will be around 0.11 mCi/ μAh .

4 Conclusions

According to this study, the Zn + p route has been shown to produce sufficient activity of $^{61,62,64,67}\text{Cu}$ (with low contamination level) to be considered for practical purposes.

This work was financially supported by the Hungarian Research Foundation (OTKA: K60223 and T048345), the Hungarian Science and Technology Foundation and the National Research Foundation (Pretoria) under a Hungarian-South African bilateral agreement (DAK 19/06), and the Japanese Society for Promotion of Sciences (Tokyo).

References

1. F. Szelecsényi, G. Blessing, S.M. Qaim, *Appl. Radiat. Isot.* **49**, 575 (1993).
2. K. Abbas, J. Kozempel, M. Bonardi, F. Groppi, A. Alfarano, U. Holzwarth, F. Simonelli, H. Hofman, W. Horstmann, E. Menapace, N. Gibson, *Appl. Radiat. Isot.* **64**, 1001 (2006).
3. F. Szelecsényi, Z. Kovács, K. Suzuki, T. Fukumura, K. Okada, K. Mukai, in *Advances in Nuclear and Radiochemistry*, edited by S.M. Qaim, H.H. Coenen, Vol. 3 (Schriften des Forschungszentrums Jülich, 2004), p. 313.
4. F. Szelecsényi, Z. Kovács, K. Suzuki, K. Okada, T.N. van der Walt, G.F. Steyn, S. Mukherjee, *J. Radioanal. Nucl. Chem.* **263**, 539 (2005).
5. F. Szelecsényi, Z. Kovács, T.N. van der Walt, G.F. Steyn, K. Suzuki, K. Okada, *Appl. Radiat. Isot.* **58**, 377 (2003).
6. F. Szelecsényi, G.F. Steyn, Z. Kovács, C. Vermeulen, N.P. van der Meulen, S.G. Dolley, T.N. van der Walt, K. Suzuki, K. Mukai, *Nucl. Instrum. Meth. B* **240**, 625 (2005).
7. F. Szelecsényi, G.F. Steyn, S.G. Dolley, Z. Kovács, C. Vermeulen, T.N. van der Walt, in *Proceedings of the 15th Pacific Basin Nuclear Conference, Sydney, Australia, 2006* (CD-ROM).
8. S.G. Dolley, T.N. van der Walt, G.F. Steyn, F. Szelecsényi, Z. Kovács, *Czechoslovak J. Phys. Suppl. D* **56**, 539 (2006).
9. T. Fukumura, K. Okada, H. Suzuki, R. Nakao, K. Mukai, F. Szelecsényi, Z. Kovács, K. Suzuki, *Nucl. Med. Biol.* **33**, 821 (2006).
10. P. Obložinský, Yu.N. Shubin, Y. Zhuang, in *International Atomic Energy Agency Report IAEA-TECDOC-1211*.